

Synthesis and spectroscopic studies of some transition metal complexes of a novel Schiff base ligands derived from 5-phenylazo-salicylaldehyde and *o*-amino benzoic acid

Moamen S. Refat^{a,*}, Ibrahim M. El-Deen^a, Hassan K. Ibrahim^b, Samir El-Ghool^a

^a Department of Chemistry, Faculty of Education, Port Said, Suez Canal University, Mohamed Ali Street, Port Said, Egypt

^b Department of Chemistry, Faculty of Science, Ismalia, Suez Canal University, Ismalia, Egypt

Received 31 October 2005; accepted 23 January 2006

Abstract

Cu(II), Mn(II), Ni(II), and Zn(II) metal complexes with novel heterocyclic Schiff base derived from 5-phenyl azo-salicylaldehyde and *o*-amino benzoic acid have been synthesized and characterized on the basis of elemental analyses, electronic, IR, and ¹H NMR spectra, and also by aid of scanning electron microscopy (SEM), X-ray powder diffraction, molar ratio measurements, molar conductivity measurements, and thermogravimetric analyses. It has been found that the Schiff base behaves as neutral tridentate (ONO) ligand forming chelates with 1:1 (metal:ligand) stoichiometry.

© 2006 Elsevier B.V. All rights reserved.

Keywords: 5-Phenyl azo-salicylaldehyde; *o*-Amino benzoic acid; Transition metals; Infrared spectra; Thermogravimetric analyses

1. Introduction

During the past two decades, considerable attention has been paid to the chemistry of the transition metal complexes of Schiff bases containing nitrogen and other donors [1–4]. The ligands, derived by the condensation of a primary amine and an active carbonyl group, contain the azomethine group [5,6]. Schiff bases are a class of important compounds in medicinal and pharmaceutical field. They show biological activities including antibacterial [7–10], antifungal [11,12], anticancer [13–15], and herbicidal [16] activities. Furthermore, Schiff bases are utilized as starting material in the synthesis of industrial [17] and biological compounds such as β -lactams [18]. Azo compounds have been used for a long time as dyes in industry [19]. In addition, azo compounds are used in analytical chemistry as indicators in pH, redox, or complexometric titration [20,21]. Some azo compounds have shown a good antibacterial activity [22,23]. The existence of an azo moiety in different types of compounds has caused them to show pesticidal activity [16]. Based on the mentioned properties for Schiff bases and azo compounds, we

reported herein the syntheses and spectroscopic studies as well as thermal investigation of a novel Schiff base derivatives ligand (H₂L) (L₁ = 2-[5-phenyl azo-2-hydroxy benzylidene amino]-benzoic acid; L₂ = 2-[5-(2-chlorophenyl) azo-2-hydroxy benzylidene amino] benzoic acid; L₃ = 2-[5-(4-methyl phenyl) azo-2-hydroxy benzylidene amino] benzoic acid) and its Cu(II), Mn(II), Ni(II), and Zn(II) complexes. Mass spectra and ¹H NMR spectra were obtained to determine the structure of the ligands HL₁, HL₂, and HL₃.

2. Experimental

2.1. Materials

o-Chloroaniline, *o*-amino benzoic acid, *p*-toluidine, salicylaldehyde, aniline, metal salts (Cu(CH₃COO)₂·3H₂O, NiSO₄·7H₂O, MnSO₄·4H₂O, and ZnSO₄·7H₂O), and other chemicals were obtained from Porlabo (reagent grade).

2.2. Synthesis of the azo compounds

Aniline (4.65 ml, 50 mmol), *o*-chloroaniline (6.40 ml, 50 mmol), or *p*-toluidine (5.35 g, 50 mmol) was mixed with hydrochloric acid (37%, 6.0 ml, 40 mmol) in distilled water

* Corresponding author.

E-mail address: msrefat@yahoo.com (M.S. Refat).

(30 ml) and diazotized below 5 °C with sodium nitrite (40.0 mmol, 2.8 g) in distilled water (30 ml). The diazotized aniline, *o*-chloroaniline, or *p*-toluidine compounds were coupled with salicylaldehyde in alkaline media below 5 °C. The pH value during the coupling was kept fixed between 7 and 9. Coupling to the salicylaldehyde occurred in basic media at the *para* position to the hydroxyl group (Scheme 1) [24].

All diazo compounds were recrystallized several times from ethyl alcohol (95%) and the addition of hydrochloric acid to pH 3. All organic impurities were then extracted by washing with small portion of diethyl ether. The precipitated compounds were dried under vacuum at 70 °C. The other, all diazo compounds (L₂ and L₃) were synthesized in the same manner. The purity of all diazo compounds was evaluated by thin layer chromatography.

2.3. Synthesis of the Schiff base ligand

The Schiff base ligands were synthesized according to the known condensation method [25]. The methanol solution (50 ml) of *o*-amino benzoic acid (6.85 g, 50 mmol) was mixed with a solution of the derivatives of 5-phenyl azo-salicylaldehyde (11.3 g, 50 mmol, L₁; 13.02 g, 50 mmol, L₂; 12.0 g, 50 mmol, L₃) in water (100 ml). The mixture was refluxed and stirred magnetically for 2 h at 70 °C on a hot plate. After cooling, the

solution of the Schiff base was filtered, and the solid was washed several times with methanol. All organic impurities were then extracted by washing with small portions of diethyl ether. The ligands were dried in vacuo over calcium chloride, and were recrystallized several times from ethyl alcohol. The purity of the ligands was evaluated by thin layer chromatography. Elemental analysis CHN, IR, UV–vis, mass, and ¹H NMR spectra confirm the composition of the ligands. The formulas of the azo-linked Schiff base ligands are given in Scheme 1.

2.4. Synthesis of metal complexes

All of the complexes were synthesized by adding of the appropriate metal salts (1.0 mmol, in 20 ml ethyl alcohol–water (1:1)) to a hot solution of the ligands (1.0 mmol, in 30 ml ethyl alcohol (95%)). The pH was adjusted to 6.00–7.00 using alcoholic sodium hydroxide (0.01 M). The resulting solutions were stirred and heated on a hot plate at 70 °C for 30 min. The volume of the obtained solution was reduced to one-half by evaporation. One day later, the colored solid of the complexes formed was filtered, the solids washed with ethanol and diethyl ether, and finally dried under vacuum. The synthesized complexes were recrystallized from ethanol–water (1:1). The purity of all complexes was evaluated by thin layer chromatography. All complexes were prepared by the same method and isolated as powdered material. Elemental analysis CHN, IR, mass spectra, UV–vis, ¹H NMR, XRD, SEM, and thermogravimetric analyses as well as atomic absorption spectra confirmed the composition of metal complexes.

2.5. Apparatus and experimental conditions

2.5.1. Elemental analysis and metal percentage

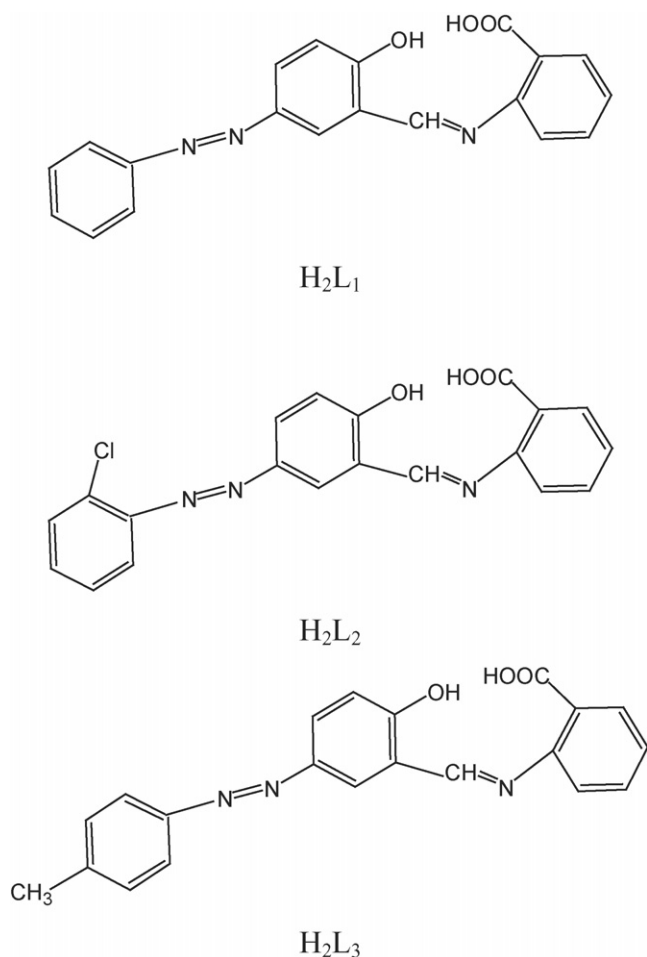
Elemental analyses (C, H, and N) were performed using a Perkin-Elmer CHN 2400 elemental analyzer. Percentages of the metal ions of the complexes were determined using PYE-UNICAM SP 1900 atomic absorption spectrophotometer supplied with the corresponding lamp used for this purpose.

2.5.2. Infrared spectra

IR spectra (4000–400 cm⁻¹) were recorded as KBr pellets on Perkin-Elmer spectrum RXI FT-IR system spectrophotometer.

2.5.3. Electronic spectra

UV spectra were measured with a Jenway 6405 spectrophotometer, using 1 cm Quartz cell, slit fixed at 2 nm. The range of wavelength was from 200 to 800 nm. The concentrations of ligands (H₂L₁, H₂L₂, and H₂L₃) were 5 × 10⁻⁴ mol/l (pH 7), each of these ligands was added into five 5 ml cuvettes, each containing 1 ml of this solution, then metal ions (Cu(II), Mn(II), Ni(II), or Zn(II)) solutions of 5 × 10⁻⁴ mol/l (regulated at pH 7) from 0 to 4.00 ml were added into cuvettes, respectively, and diluted to 5 ml with ethanol (95%). The final concentration of ligands was 10⁻⁴ mol/l in each cuvette, the final concentrations of metal ions were 0.00, 0.25 × 10⁻⁴, 0.50 × 10⁻⁴, 0.75 × 10⁻⁴, 1.00 × 10⁻⁴, 1.50 × 10⁻⁴, 2.00 × 10⁻⁴, 2.50 × 10⁻⁴, 3.00 × 10⁻⁴, 3.50 × 10⁻⁴, and 4.00 × 10⁻⁴ mol/l. Until equilibrium was reached, each UV absorption was recorded.



Scheme 1. Azo-linked Schiff base ligands.

2.5.4. ^1H NMR spectra

The structures of ligands (H_2L_1 , H_2L_2 , and H_2L_3) and complexes were elucidated using a Varian Gemini 200 MHz ^1H NMR spectrometer. The solvent used was DMSO. The internal reference was the peak due to the solvent. Ligands and solid complex were added into sample tubes and dissolved in DMSO, respectively. The ^1H NMR was done at 25°C .

2.5.5. Thermal analysis (TG) and DTG techniques

Thermogravimetric analyses (TG) were carried out in the temperature range from 25 to 800°C in a stream of nitrogen atmosphere by Shimadzu TGA 50H thermal analysis. The experimental conditions were: aluminum crucible with 1 mg sample, nitrogen atmosphere with a 30 ml/min flow rate, and a heating rate $15^\circ\text{C}/\text{min}$.

2.5.6. Mass spectra

The purity of (H_2L_1 , H_2L_2 , and H_2L_3) is checked from mass spectra at 70 eV by using AEI MS 30 mass spectrometer.

2.5.7. X-ray powder diffraction

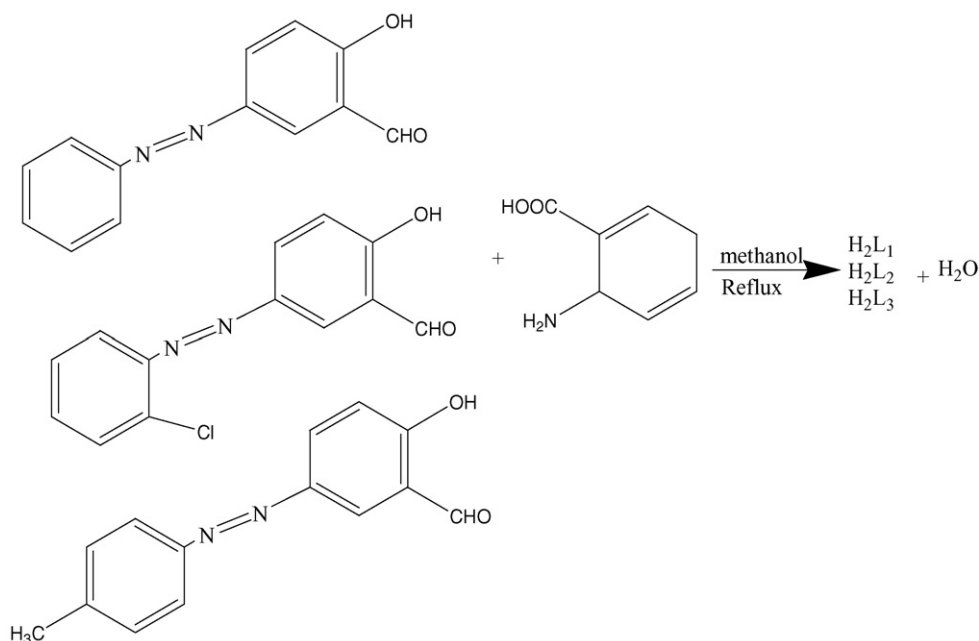
The X-ray powder diffraction analyses were carried out by using Rigaku Model ROTAFLEX Ru-200. Radiation was provided by copper target (Cu anode 2000 W) high intensity X-ray tube operated at 40 kV and 35 MA. Divergence slit and the receiving slit were 1 and 0.1, respectively.

2.5.8. Scanning electron microscope

The scanning electron microscope (SEM) images were taken in JEOL-840 equipment, with an accelerating voltage of 15 kV.

3. Results and discussion

Condensation of the 5-phenyl azo salicylaldehyde and its derivatives with *o*-amino benzoic acid readily gives rise to the corresponding imine H_2L_1 , H_2L_2 , and H_2L_3 , which was easily identified by its IR, ^1H NMR and mass spectra.



Tetradentate complexes were obtained upon reaction between metal ions and H_2L_1 , H_2L_2 , and H_2L_3 ligands at 1:1 molar ratio. The ligands H_2L_1 , H_2L_2 , and H_2L_3 , on reaction with $\text{Cu}(\text{CH}_3\text{COO})_2 \cdot 3\text{H}_2\text{O}$, $\text{NiSO}_4 \cdot 7\text{H}_2\text{O}$, $\text{MnSO}_4 \cdot 4\text{H}_2\text{O}$, and $\text{ZnSO}_4 \cdot 7\text{H}_2\text{O}$ salts, yield complexes corresponding to the general formula $[\text{CuL}_1] \cdot 2\text{H}_2\text{O}$ (**1**), $[\text{MnL}_1] \cdot 4\text{H}_2\text{O}$ (**2**), $[\text{NiL}_1] \cdot 3\text{H}_2\text{O}$ (**3**), $[\text{ZnL}_1] \cdot 5\text{H}_2\text{O}$ (**4**), $[\text{CuL}_2] \cdot 4\text{H}_2\text{O}$ (**5**), $[\text{MnL}_2] \cdot 3\text{H}_2\text{O}$ (**6**), $[\text{NiL}_2] \cdot 4\text{H}_2\text{O}$ (**7**), $[\text{ZnL}_2] \cdot 4\text{H}_2\text{O}$ (**8**), $[\text{CuL}_3] \cdot 3\text{H}_2\text{O}$ (**9**), $[\text{MnL}_3] \cdot 4\text{H}_2\text{O}$ (**10**), $[\text{NiL}_3] \cdot 2\text{H}_2\text{O}$ (**11**), and $[\text{ZnL}_3] \cdot 3\text{H}_2\text{O}$ (**12**).

The newly synthesized Schiff base ligands and its complexes are very stable at room temperature in the solid state. The ligands are insoluble in common organic solvents in cold or hot conditions. But the ligands and its metal complexes are generally soluble in DMF and DMSO. The colors, yield, melting/decomposition points, elemental analyses, and molar conductances of H_2L_1 , H_2L_2 , H_2L_3 , and **1–12** complexes are presented in Table 1. The analytical data are in a good agreement with the proposed stoichiometry of the complexes.

The metal-to-ligand ratio in the Cu(II), Mn(II), Ni(II), and Zn(II) complexes was found to be 1:1. All the complexes (**1–12**) have two, three, four, or five molecules of water of crystallization.

The molar conductivity values for all the complexes in aqueous medium (10^{-3} M) were in the range of $4\text{--}15\ \Omega^{-1}\text{ cm}^2\text{ mol}^{-1}$, suggesting them to be non-electrolytes (Table 1). The ligands decomposed at temperatures higher than 200°C , while all complexes decomposed at temperatures higher than 250°C . All of the new complexes and Schiff base seemed to have dye character due to the high molar extinction constant. Elemental analyses were in good agreement with those required for the purpose of formula. According to the elemental analyses, IR, UV-vis, ^1H NMR, and thermogravimetric data, the complexes of the tridentate ligands had one coordinated water molecule. Analytical data for all ligands and complexes are listed in Table 1.

Table 1
Elemental analyses and physical data of ligands H₂L₁, H₂L₂, H₂L₃, and their complexes 1–12

Complexes	Empirical formula	Molecular weight (g/mol)	Color	Melting point	Content ((calculated) found)			Yield	Λ_m ($\Omega \text{ cm}^2 \text{ mol}^{-1}$)
					%C	%H	%N		
H ₂ L ₁	C ₂₀ H ₁₄ N ₃ O ₃	344	Pink	236	(69.77) 69.82	(4.07) 4.02	(12.71) 12.18	73	2.7
H ₂ L ₂	C ₂₀ H ₁₃ N ₃ O ₃ Cl	378.5	Red	252	(63.41) 63.11	(3.43) 3.38	(11.10) 10.59	77	3.1
H ₂ L ₃	C ₂₁ H ₁₆ N ₃ O ₃	358	Orange	262	(70.39) 70.13	(4.47) 4.41	(11.73) 11.64	71	2.4
[CuL ₁]-2H ₂ O	C ₂₀ H ₁₆ N ₃ O ₅ Cu	441.55	Olivey green	>387	(54.35) 54.70	(3.62) 3.57	(9.51) 9.36	64	5.3
[MnL ₁]-4H ₂ O	C ₂₀ H ₂₀ N ₃ O ₇ Mn	468.94	Violet	>350	(51.18) 51.03	(4.62) 4.18	(8.95) 8.79	63	4.2
[NiL ₁]-3H ₂ O	C ₂₀ H ₁₈ N ₃ O ₆ Ni	454.70	Yellow	>400	(52.78) 52.90	(3.96) 3.88	(9.23) 9.11	62	10.3
[ZnL ₁]-5H ₂ O	C ₂₀ H ₂₂ N ₃ O ₈ Zn	497.38	Orange	>400	(48.25) 48.10	(4.42) 4.37	(8.44) 8.33	66	12.5
[CuL ₂]-4H ₂ O	C ₂₀ H ₁₉ N ₃ O ₇ ClCu	512.05	Olivey green	>392	(46.87) 46.80	(3.71) 3.65	(8.20) 8.10	63	11.7
[MnL ₂]-3H ₂ O	C ₂₀ H ₁₇ N ₃ O ₆ ClMn	485.44	Violet	>400	(49.44) 49.17	(3.50) 3.44	(8.65) 8.56	60	13.3
[NiL ₂]-4H ₂ O	C ₂₀ H ₁₉ N ₃ O ₇ ClNi	507.20	Orange	>400	(47.32) 47.11	(3.74) 3.66	(8.28) 8.16	66	14.9
[ZnL ₂]-4H ₂ O	C ₂₀ H ₁₉ N ₃ O ₇ ClZn	513.88	Orange	>400	(46.79) 46.53	(3.69) 3.56	(8.17) 8.08	64	10.2
[CuL ₃]-3H ₂ O	C ₂₁ H ₂₀ N ₃ O ₆ Cu	473.55	Olivey green	>322	(53.21) 52.91	(4.22) 4.09	(8.87) 8.77	67	11.2
[MnL ₃]-4H ₂ O	C ₂₁ H ₂₂ N ₃ O ₇ Mn	482.94	Violet	>400	(52.18) 51.70	(4.55) 4.51	(8.69) 8.54	65	12.2
[NiL ₃]-2H ₂ O	C ₂₁ H ₁₈ N ₃ O ₅ Ni	450.70	Yellow	>400	(55.91) 55.73	(3.99) 3.89	(9.32) 9.13	65	14.1
[ZnL ₃]-3H ₂ O	C ₂₁ H ₂₀ N ₃ O ₆ Zn	475.38	Yellow	>400	(53.01) 52.84	(4.21) 4.18	(8.83) 8.67	62	13.7

3.1. Infrared spectra

Table 2 presents the most important IR spectral bounds for H₂L₁, H₂L₂, H₂L₃, and all the metal complexes. The functional groups of the azo-linked Schiff base ligands and the metal complexes have been appeared by infrared spectra, as given in Figs. 1–3. When the carboxylic acid group in the ligands is converted to the complexes, the absorption bands of stretching vibration of C=O group, $\nu_{\text{C=O}}$, of COOH group at about $\sim 1700 \text{ cm}^{-1}$ disappear, whereas the bands assigned to asymmetric vibrations $\nu_{\text{as}}(\text{OCO})$ at $1560\text{--}1523 \text{ cm}^{-1}$ and the bands of symmetric vibrations $\nu_{\text{s}}(\text{OCO})$ at $1395\text{--}1333 \text{ cm}^{-1}$ appear. The bands at $1627\text{--}1620 \text{ cm}^{-1}$ were assigned to the stretching vibration of the azomethine group of the ligands H₂L₁, H₂L₂, and H₂L₃. This band is shifted in the complexes toward lower frequencies because of the coordination of the nitrogen to the metal ion [26]. This fact can be explained by the withdrawing

of electrons from nitrogen atom to the metal ion due to coordination. The infrared spectra of the complexes exhibited broad bands at $3425\text{--}3394 \text{ cm}^{-1}$ that are attributed to OH of the crystal water molecules, while the bands observed at approximately $839\text{--}819 \text{ cm}^{-1}$ are assigned to coordinated water molecule [27]. The infrared spectra of azo-linked Schiff base ligands showed bands around $1285\text{--}1260 \text{ cm}^{-1}$ assigned to the phenolic C–O vibration. However, in the spectra of the metal complexes, the C–O band shifted to the lower region ($\sim 1200 \text{ cm}^{-1}$). In the infrared spectra of the complexes, bands assigned to M–N and M–O were identified at $564\text{--}496$ and $435\text{--}415 \text{ cm}^{-1}$, respectively [28] (Figs. 1–3).

3.2. Molar conductivities of metal chelates

Conductivity measurements in non-aqueous solutions have frequently been used in structural studies of metal chelates

Table 2
Infrared spectral data for the azo-linked Schiff base ligands and their complexes (cm^{-1})

Compounds	$\nu(\text{OH})$ hydrated water	$\nu(\text{OH})$ coordinated H ₂ O	$\nu(\text{C=O})$ COOH ⁻	$\nu(\text{C=N})$	$\nu_{\text{as}}(\text{C-O})$ COO ⁻	$\nu_{\text{s}}(\text{C-O})$ COO ⁻	$\nu(\text{C-O})$ phenolic	$\nu(\text{M-N})$	$\nu(\text{M-O})$
H ₂ L ₁	3472 br	–	1682 mw	1620 vs	–	–	1260 w	–	–
[CuL ₁]-2H ₂ O	3421 br	837 s	–	1616 vs	1523 ms	1392 vs	1191 ms	529 w	423 ms
[MnL ₁]-4H ₂ O	3425 br	837 s	–	1618 vs	1526 s	1395 vs	1186 ms	518 w	424 w
[NiL ₁]-3H ₂ O	3424 br	837 ms	–	1615 vs	1540 s	1379 s	1184 ms	523 vw	415 vw
[ZnL ₁]-5H ₂ O	3424 br	819 s	–	1618 vs	1538 vs	1379 s	1186 s	496 w	435 vw
H ₂ L ₂	3444 br	–	1700 w	1621 vs	–	–	1285 ms	–	–
[CuL ₂]-4H ₂ O	3425 s	837 s	–	1609 vs	1554 s	1394 s	1247 w	527 w	426 ms
[MnL ₂]-3H ₂ O	3425 br	836 ms	–	1618 vs	1558 s	1395 s	1254 vw	536 w	418 vw
[NiL ₂]-4H ₂ O	3394 br	838 s	–	1613 s	1532 vs	1388 vs	1257 w	524 s	416 w
[ZnL ₂]-4H ₂ O	3425 br	825 s	–	1591 vs	1537 vs	1379 s	1262 w	532 s	423 vw
H ₂ L ₃	3424 br	–	1698 w	1627 vs	–	–	1285 w	–	–
[CuL ₃]-3H ₂ O	3424 br	838 s	–	1624 vs	1552 vs	1382 vs	1246 w	519 s	422 s
[MnL ₃]-4H ₂ O	3424 br	838 ms	–	1623 vs	1560 w	1394 s	1252 vw	517 vs	419 s
[NiL ₃]-2H ₂ O	3425 br	839 s	–	1620 vs	1528 s	1333 s	1255 ms	516 ms	423 vw
[ZnL ₃]-3H ₂ O	3423 br	825 s	–	1593 vs	1537 vs	1377 s	1221 ms	546 ms	433 vw

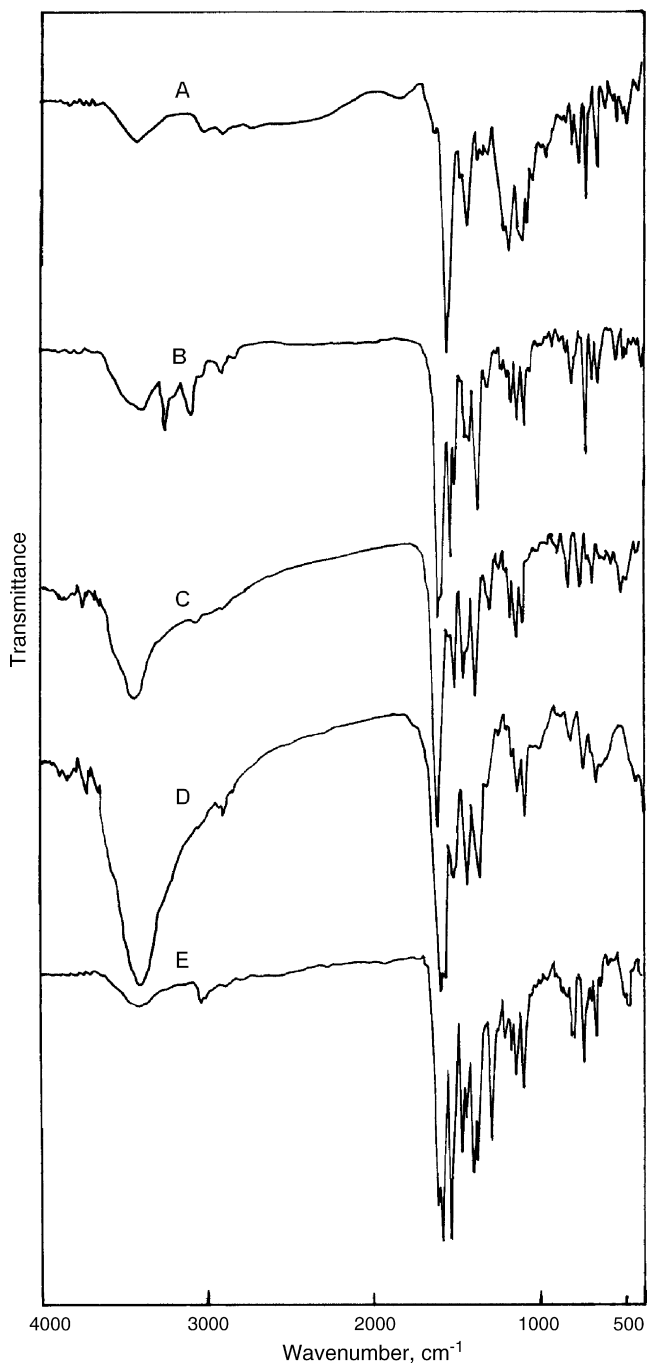


Fig. 1. Infrared spectra of: (A) H_2L_1 , (B) $[CuL_1] \cdot 2H_2O$ (1), (C) $[MnL_1] \cdot 4H_2O$ (2), (D) $[NiL_1] \cdot 3H_2O$ (3), and (E) $[ZnL_1] \cdot 5H_2O$ (4).

within the limits of their solubility. They provide a method of testing the degree of ionization of the complexes, the molar ions that a complex liberates in solution, the higher will be its molar conductivity and vice versa. The non-ionized complexes have negligible value of molar conductance. The molar conductivities of the solid chelates are measured for 10^{-3} mol solution of 1:1 complexes in DMSO. The conductivity data reported for these complexes are given in Table 1. The product of the cell constant and the measured conductance of a solution gives the specific conductivity K . The molar conductance ($\Omega^{-1} \text{ cm}^2 \text{ mol}^{-1}$) is

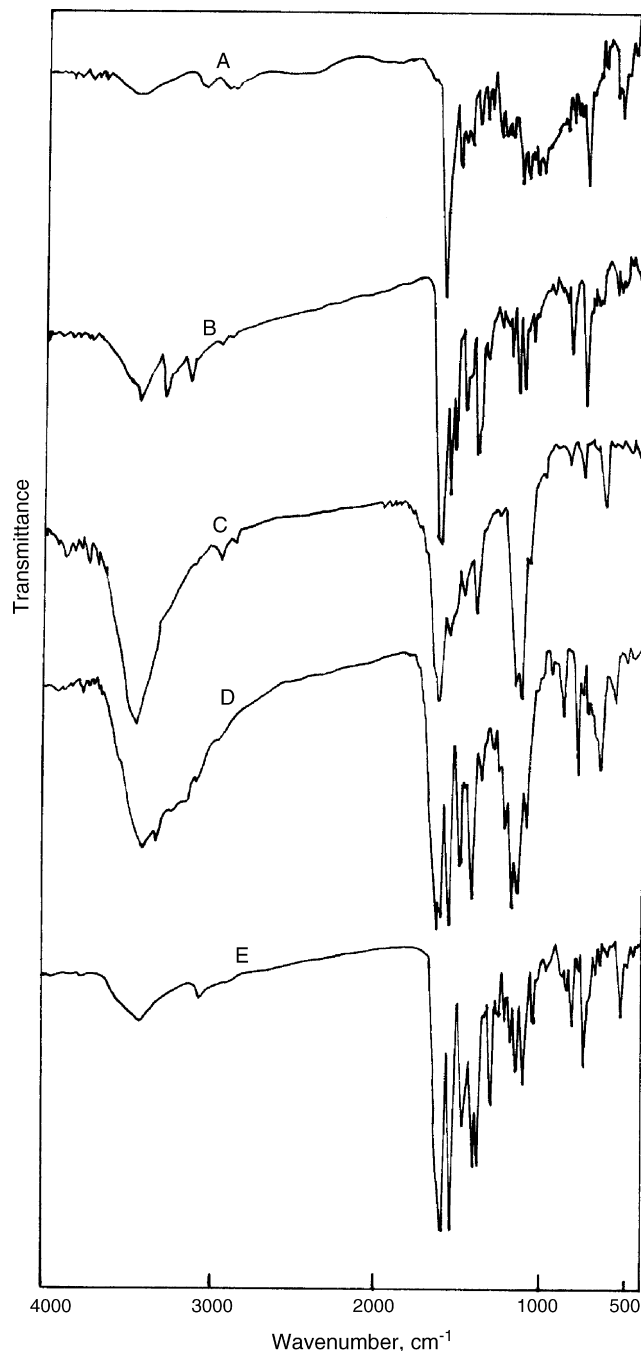


Fig. 2. Infrared spectra of: (A) H_2L_2 , (B) $[CuL_2] \cdot 4H_2O$ (5), (C) $[MnL_2] \cdot 3H_2O$ (6), (D) $[NiL_2] \cdot 4H_2O$ (7), and (E) $[ZnL_2] \cdot 4H_2O$ (8).

given by the relation:

$$\Lambda_m = \frac{K}{C} \times 1000$$

where C (mol/l) is the concentration of the solution. It is clear from the conductivity data that the complexes present behave as weak electrolytes. Also the molar conductance values indicate that the anions may be present inside the coordination sphere or absent. This result was confirmed from the chemical analysis where CH_3COO^- or SO_4^{2-} ions are not precipitated colored

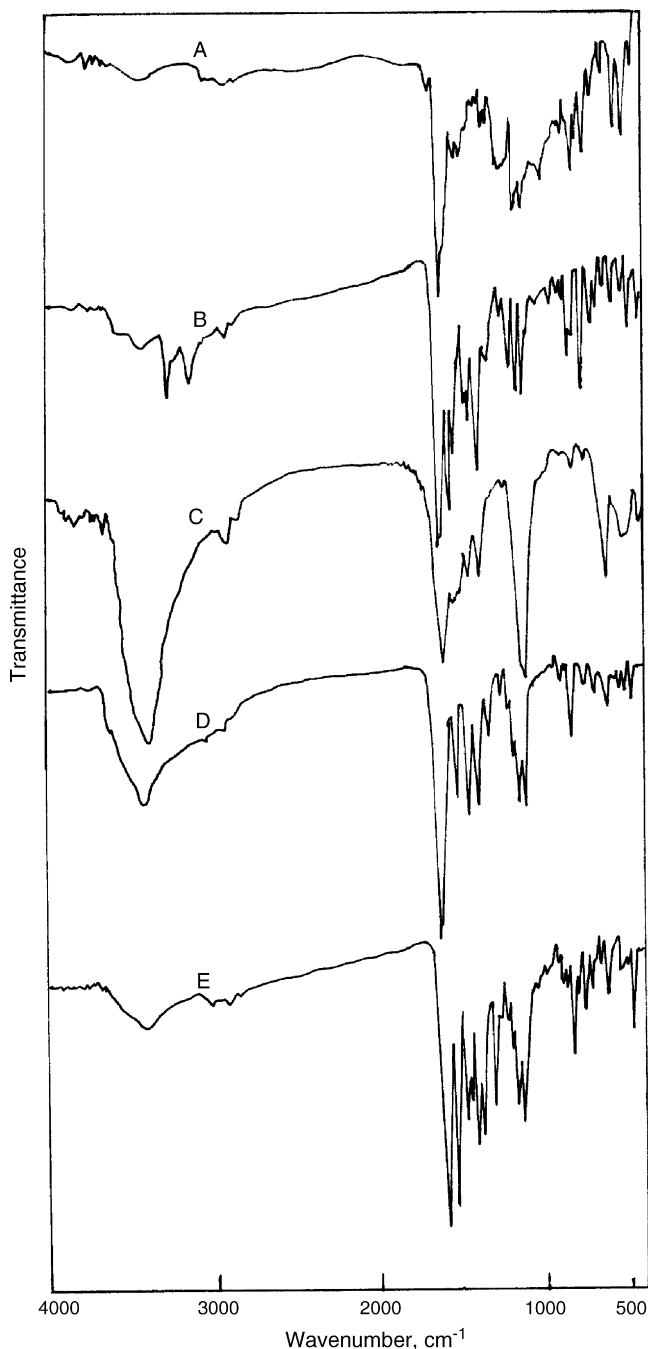


Fig. 3. Infrared spectra of: (A) H_2L_3 , (B) $[CuL_3] \cdot 3H_2O$ (9), (C) $[MnL_3] \cdot 4H_2O$ (10), (D) $[NiL_3] \cdot 2H_2O$ (11), and (E) $[ZnL_3] \cdot 3H_2O$ (12).

by addition of $FeCl_3$ or $BaCl_2$ solutions, respectively. All the complexes did not show electrolytic properties. This fact elucidated that the CH_3COO^- and SO_4^{2-} are absent, and that one of the water molecules completes the coordination sphere of the studied complexes.

3.3. Electronic spectra

Table 3 shows the absorption values of L_1 , L_2 , and L_3 at ~ 370 nm with the addition of Cu(II), Mn(II), Ni(II), and Zn(II) solution to it. UV spectra (Fig. 4) clearly indicated a

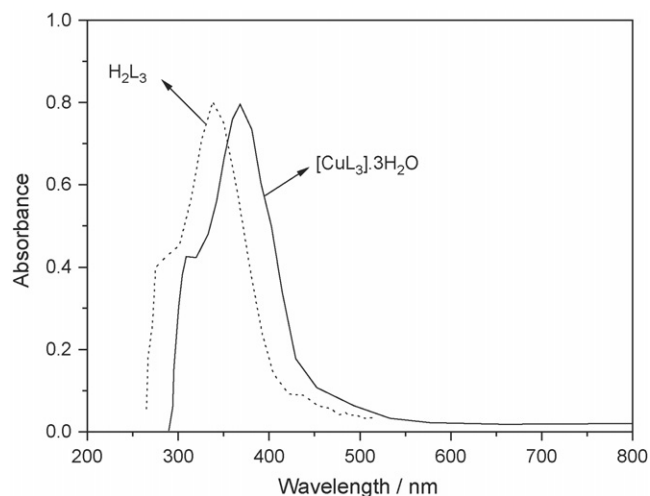


Fig. 4. Electronic spectra of H_2L_3 and its copper complex.

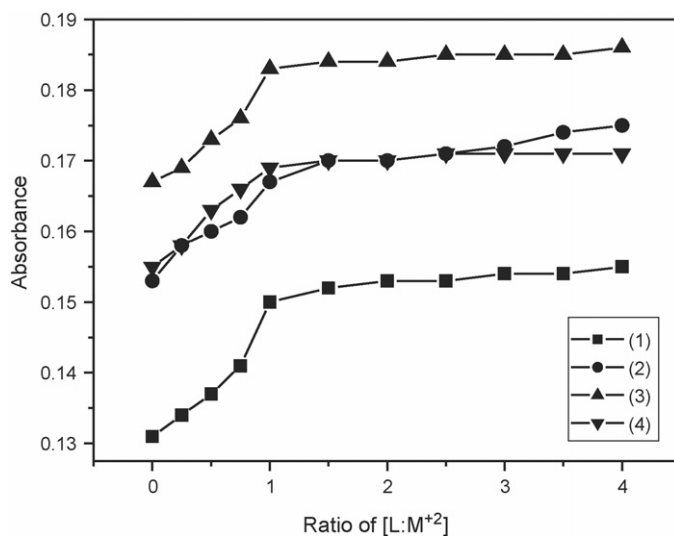


Fig. 5. The relationship of absorption of H_2L_1 with the addition of Cu(II) [1], Mn(II) [2], Ni(II) [3], and Zn(II) [4] solution.

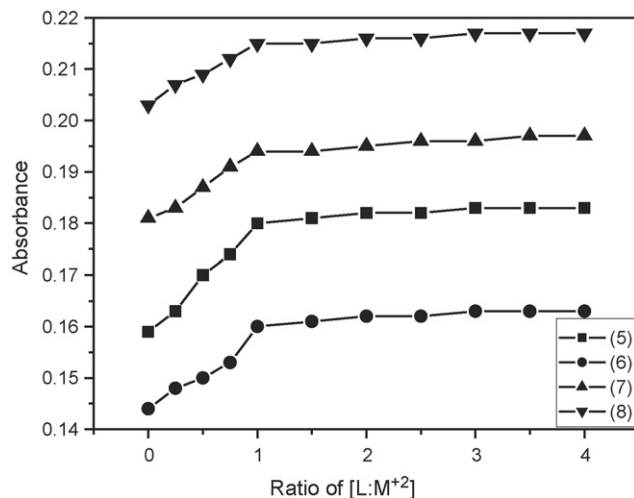


Fig. 6. The relationship of absorption of H_2L_2 with the addition of Cu(II) [5], Mn(II) [6], Ni(II) [7], and Zn(II) [8] solution.

Table 3
Absorption data of ligands (L_1 , L_2 , and L_3) solution with the addition of metal M^{2+} ($M^{2+} = \text{Cu, Mn, Ni, and Zn}$) solution, where $[\text{CuL}_1] \cdot 2\text{H}_2\text{O}$ (1), $[\text{MnL}_1] \cdot 4\text{H}_2\text{O}$ (2), $[\text{NiL}_1] \cdot 3\text{H}_2\text{O}$ (3), $[\text{ZnL}_1] \cdot 5\text{H}_2\text{O}$ (4), $[\text{CuL}_2] \cdot 4\text{H}_2\text{O}$ (5), $[\text{MnL}_2] \cdot 3\text{H}_2\text{O}$ (6), $[\text{NiL}_2] \cdot 4\text{H}_2\text{O}$ (7), $[\text{ZnL}_2] \cdot 4\text{H}_2\text{O}$ (8), $[\text{CuL}_3] \cdot 3\text{H}_2\text{O}$ (9), $[\text{MnL}_3] \cdot 4\text{H}_2\text{O}$ (10), $[\text{NiL}_3] \cdot 2\text{H}_2\text{O}$ (11), and $[\text{ZnL}_3] \cdot 3\text{H}_2\text{O}$ (12)

Molar ratio, $L:M^{2+}$	Concentration of L_n (10^{-4} ml/l)	Concentration of M^{2+} (10^{-4} ml/l)	1	2	3	4	5	6	7	8	9	10	11	12
0	1.00	0	0.131	0.153	0.167	0.155	0.159	0.144	0.181	0.203	0.147	0.182	0.211	0.191
1:0.25	1.00	0.25	0.134	0.158	0.169	0.158	0.163	0.148	0.183	0.207	0.149	0.186	0.214	0.195
1:0.50	1.00	0.50	0.137	0.160	0.173	0.163	0.170	0.150	0.187	0.209	0.153	0.189	0.216	0.194
1:0.75	1.00	0.75	0.141	0.162	0.176	0.166	0.174	0.153	0.191	0.212	0.155	0.191	0.219	0.201
1:1.00	1.00	1.00	0.150	0.167	0.183	0.169	0.180	0.160	0.194	0.215	0.158	0.193	0.221	0.205
1:1.50	1.00	1.50	0.152	0.170	0.184	0.170	0.181	0.161	0.194	0.215	0.162	0.193	0.222	0.206
1:2.00	1.00	2.00	0.153	0.170	0.184	0.170	0.182	0.162	0.195	0.216	0.162	0.193	0.222	0.206
1:2.50	1.00	2.50	0.153	0.171	0.185	0.171	0.182	0.162	0.196	0.216	0.163	0.194	0.222	0.207
1:3.00	1.00	3.00	0.154	0.172	0.185	0.171	0.183	0.163	0.196	0.217	0.163	0.195	0.222	0.207
1:3.50	1.00	3.50	0.154	0.174	0.185	0.171	0.183	0.163	0.197	0.217	0.163	0.195	0.223	0.207
1:4.00	1.00	4.00	0.155	0.175	0.186	0.171	0.183	0.163	0.197	0.217	0.164	0.195	0.223	0.207

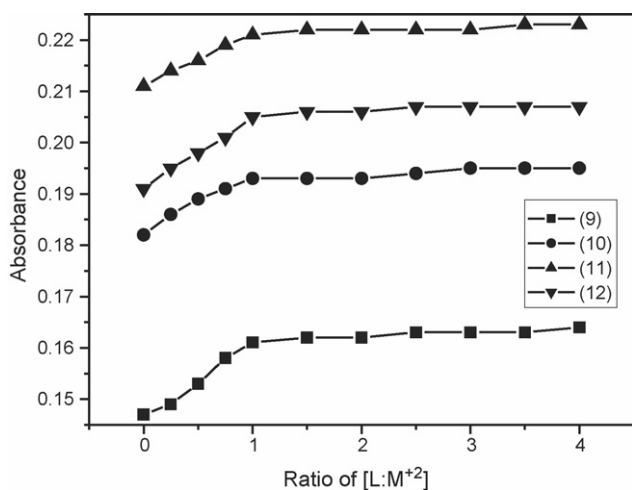


Fig. 7. The relationship of absorption of H_2L_3 with the addition of Cu(II) [9], Mn(II) [10], Ni(II) [11], and Zn(II) [12] solution.

bathochromic shift (red shift) for the two detected peaks in the L_3 as one of the studied ligands from 340 and 280 to 370 and 300 nm. We plot the curves according to the data listed in Table 3. From Table 3 and Figs. 5–7, we can see absorption values were enhanced with increasing concentration of Cu(II) , Mn(II) , Ni(II) , and Zn(II) at the beginning and then formed a platform, when $L:M^{2+}$ is about 1:1. This fact illustrated that 1 mol ligand (L_1 , L_2 , and/or L_3) molecules will coordinate with 1 mol of M^{2+} ($M^{2+} = \text{Cu, Mn, Ni, and/or Zn}$).

3.4. Mass spectra

The purity of ligands L_1 , L_2 , and L_3 is checked from mass spectra (Fig. 8A–C) where the spectra showed that a clearly base peaks (m/e) molecular weights and the intensity (%) of the three ligands ($L_1 = 2$ -[5-phenyl azo-2-hydroxy benzylidene amino]-benzoic acid, $L_2 = 2$ -[5-(2-chlorophenyl)azo-2-hydroxy benzylidene amino] benzoic acid, and $L_3 = 2$ -[5-(4-

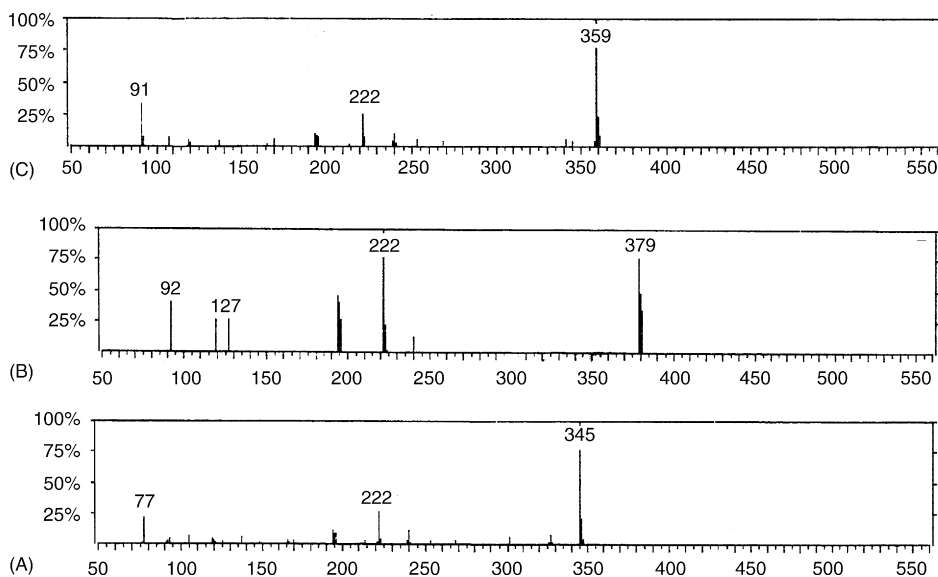


Fig. 8. Mass spectra of: (A) H_2L_1 , (B) H_2L_2 , and (C) H_2L_3 compounds.

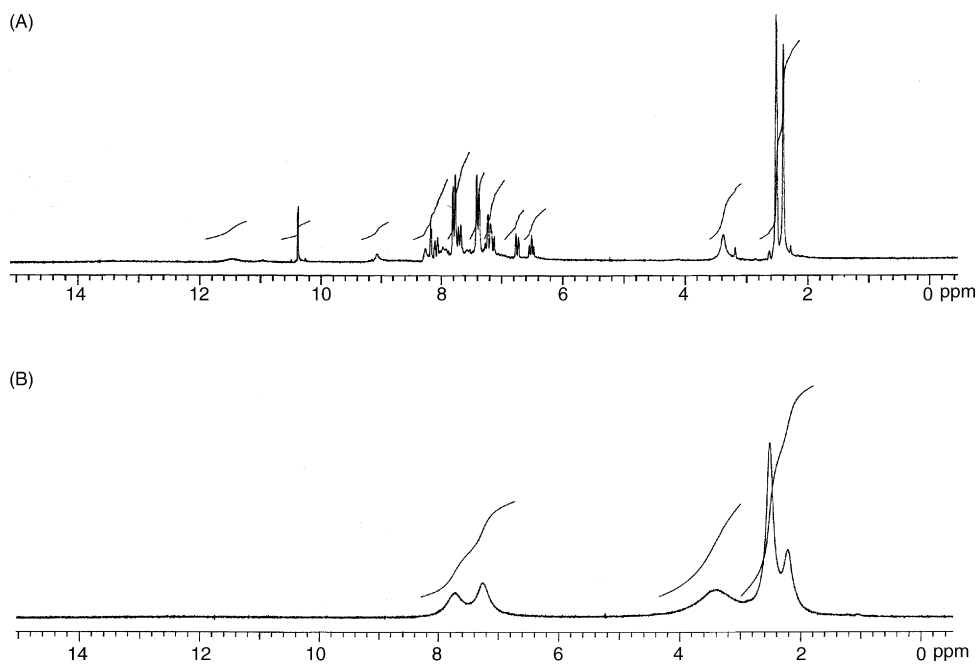


Fig. 9. ^1H NMR spectra of: (A) H_2L_3 and (B) $[\text{CuL}_3]\cdot 3\text{H}_2\text{O}$ compounds.

methyl phenyl)azo-2-hydroxy benzylidene amino] benzoic acid) at 345 (75%), 379 (80%), and 359 (83%), respectively.

3.5. ^1H NMR spectra

For instance, the ^1H NMR spectra of HL_3 (2-[5-(4-methyl phenyl) azo-2-hydroxy benzylidene amino] benzoic acid) and

its Cu(II) complex are shown in Fig. 9. The ^1H NMR spectra of the ligand, HL_3 , and the Cu(II) complex were recorded using $\text{DMSO}-d_6$ as a solvent. As a result of the ^1H NMR spectral studies, important class concerning the geometry of azo-linked Schiff base ligands was obtained. The ^1H NMR spectrum of HL_3 showed a singlet at 2.50 ppm that was assigned to the protons of methyl group, and multiplets at 6.50–8.20 ppm were assigned to

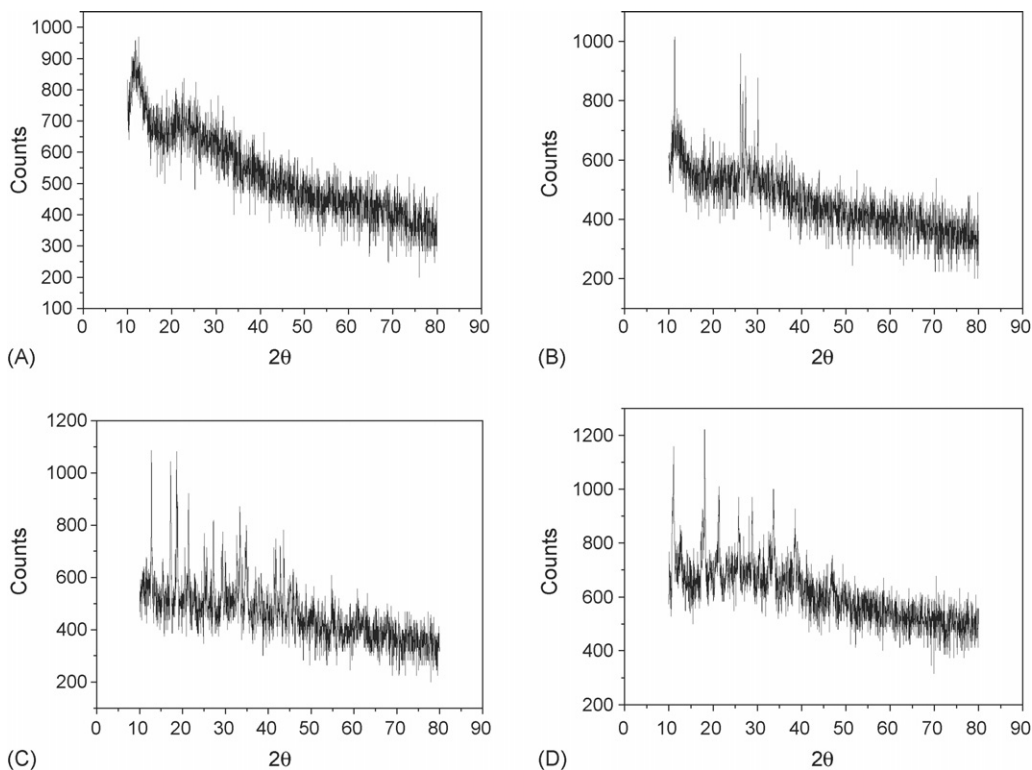


Fig. 10. XRD diagrams of: (A) $[\text{CuL}_3]\cdot 3\text{H}_2\text{O}$ (**9**), (B) $[\text{MnL}_3]\cdot 4\text{H}_2\text{O}$ (**10**), (C) $[\text{NiL}_3]\cdot 2\text{H}_2\text{O}$ (**11**), and (D) $[\text{ZnL}_3]\cdot 3\text{H}_2\text{O}$ (**12**).

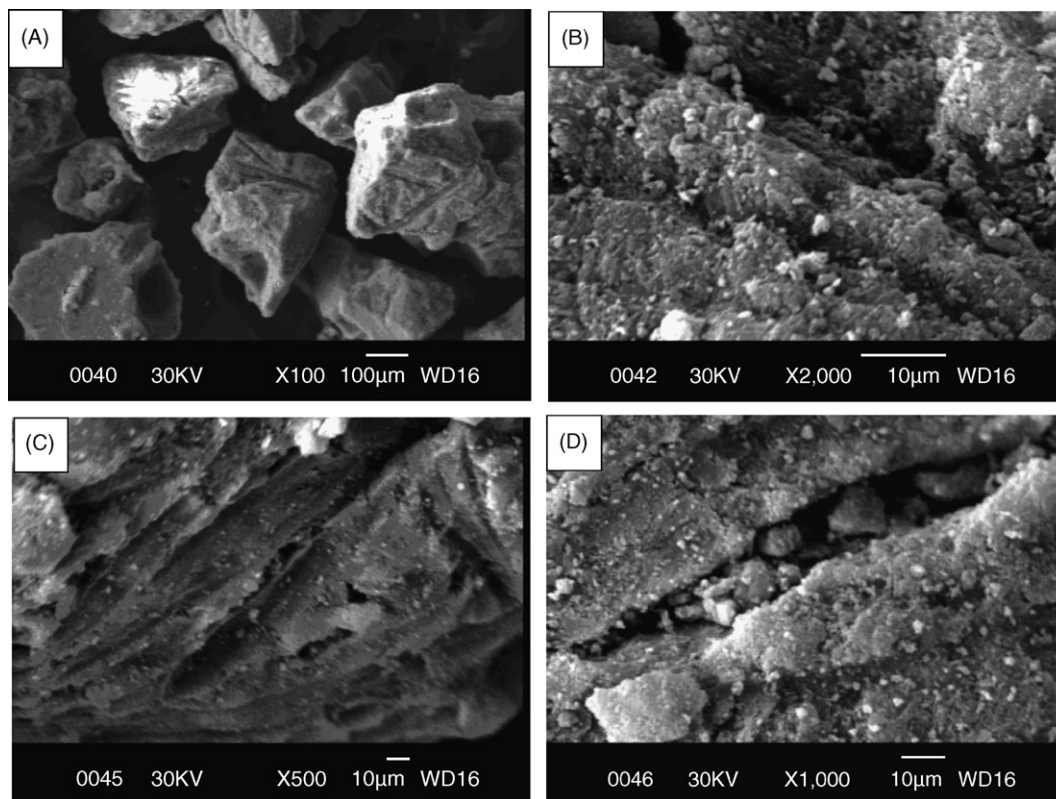
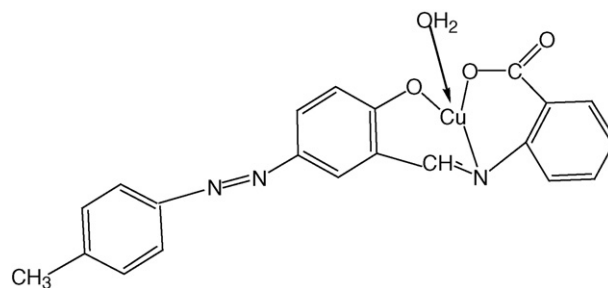


Fig. 11. SEM diagrams of: (A) $[\text{CuL}_3] \cdot 3\text{H}_2\text{O}$ (**9**), (B) $[\text{MnL}_3] \cdot 4\text{H}_2\text{O}$ (**10**), (C) $[\text{NiL}_3] \cdot 2\text{H}_2\text{O}$ (**11**), and (D) $[\text{ZnL}_3] \cdot 3\text{H}_2\text{O}$ (**12**).

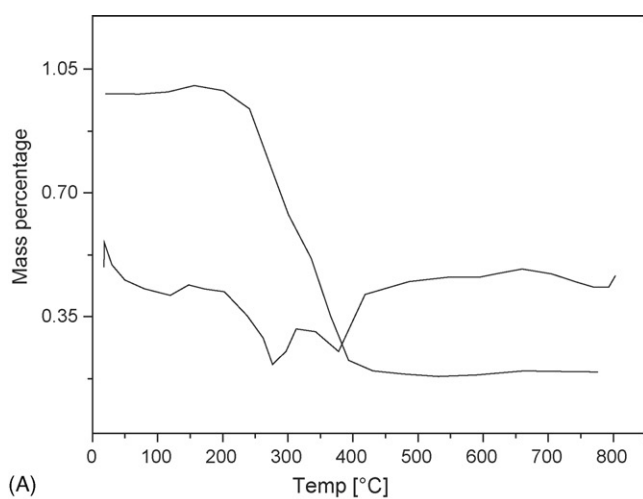
Table 4
Thermal decomposition of the metal complexes (**1–12**)

Complexes	Step	ΔT ($^{\circ}\text{C}$)	Weight loss (calculated/found) (%)	Residue (calculated/found) (%)
$[\text{CuL}_1 \cdot \text{H}_2\text{O}] \cdot \text{H}_2\text{O}$ (1)	1	60–150	4.08/3.83	CuO (18.02/19.41)
	2	150–550	77.9/76.76	
$[\text{MnL}_1 \cdot \text{H}_2\text{O}] \cdot 3\text{H}_2\text{O}$ (2)	1	50–167	7.68/7.02	MnO_2 (18.54/19.35)
	2	167–600	73.78/72.98	
$[\text{NiL}_1 \cdot \text{H}_2\text{O}] \cdot 2\text{H}_2\text{O}$ (3)	1	50–208	7.92/7.05	NiO (16.43/15.79)
	2	208–550	75.65/77.16	
$[\text{ZnL}_1 \cdot \text{H}_2\text{O}] \cdot 4\text{H}_2\text{O}$ (4)	1	90–250	14.47/14.07	ZnO (16.36/17.36)
	2	250–600	69.17/68.57	
$[\text{CuL}_2 \cdot \text{H}_2\text{O}] \cdot 3\text{H}_2\text{O}$ (5)	1	60–170	3.52/3.37	CuO (15.54/15.63)
	2	170–260	7.03/7.86	
	3	260–600	73.91/73.14	
$[\text{MnL}_2 \cdot \text{H}_2\text{O}] \cdot 2\text{H}_2\text{O}$ (6)	1	55–235	7.41/8.01	MnO_2 (17.91/18.43)
	2	235–665	74.68/73.56	
$[\text{NiL}_2 \cdot \text{H}_2\text{O}] \cdot 3\text{H}_2\text{O}$ (7)	1	75–260	10.65/10.35	NiO (4.73/15.52)
	2	260–620	74.62/74.13	
$[\text{ZnL}_2 \cdot \text{H}_2\text{O}] \cdot 3\text{H}_2\text{O}$ (8)	1	50–220	3.50/3.48	ZnO (15.84/16.40)
	2	220–627	80.66/80.12	
$[\text{CuL}_3 \cdot \text{H}_2\text{O}] \cdot 2\text{H}_2\text{O}$ (9)	1	50–275	7.60/7.27	CuO (16.80/17.27)
	2	275–640	75.60/75.46	
$[\text{MnL}_3 \cdot \text{H}_2\text{O}] \cdot 3\text{H}_2\text{O}$ (10)	1	50–200	3.72/3.77	MnO_2 (18.00/18.13)
	2	200–300	7.45/7.54	
	3	300–600	70.83/70.56	
$[\text{NiL}_3 \cdot \text{H}_2\text{O}] \cdot \text{H}_2\text{O}$ (11)	1	50–220	3.99/2.26	NiO (16.57/16.48)
	2	220–615	79.44/81.26	
$[\text{ZnL}_3 \cdot \text{H}_2\text{O}] \cdot 2\text{H}_2\text{O}$ (12)	1	70–300	7.57/7.83	ZnO (17.14/17.24)
	2	300–625	75.31/74.93	

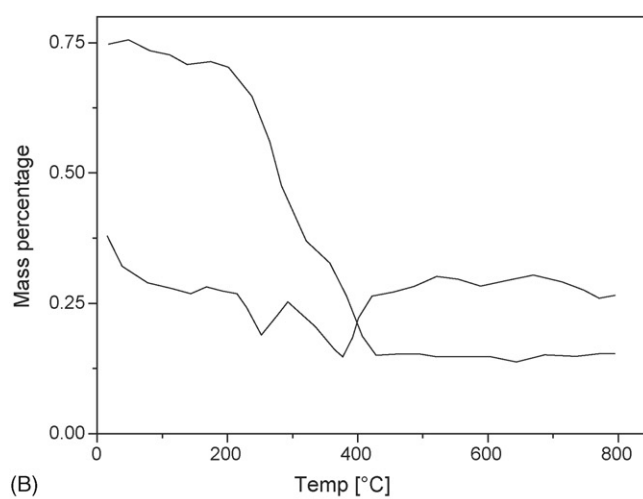
the aromatic protons. The singlet at 9.07 ppm was attributed to the proton of the azomethine group [3]. The signal of the OH-proton in the salicylaldehyde ring was observed at 10.37 ppm. A broad peak at 11.43 ppm was attributed to the OH-proton of carboxylic acid. By making comparison between the ^1H NMR data of HL_3 and its $\text{Cu}(\text{II})$ complex the mode of coordination in between the ligands and metal ions was clarified. Through the discussion of ^1H NMR spectrum of $\text{Cu}(\text{II})$ complex, we find that the peaks (signals) specialized to OH-proton of carboxylic acid and OH-proton in salicylaldehyde ring disappeared and notified the appearance of new strong broad peak at 3.38 ppm; this can be assigned to the H-proton of H_2O , which attached to the $\text{Cu}(\text{II})$ metal to complete the coordination sphere as follows:



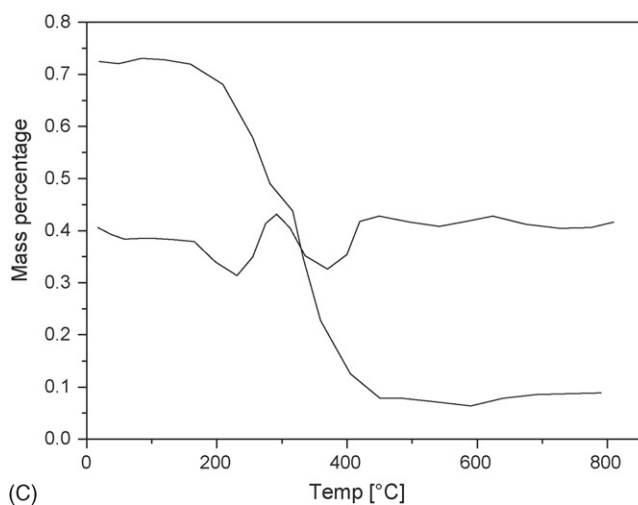
The coordination mode of $\text{Cu}(\text{II})\text{-HL}_3$



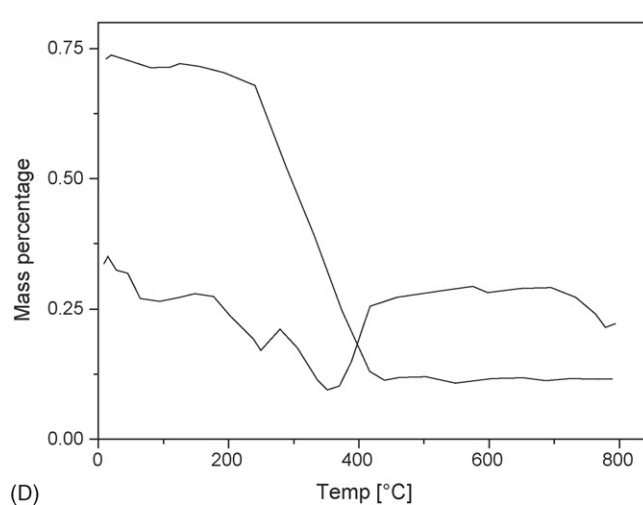
(A)



(B)



(C)



(D)

Fig. 12. TGA diagrams of: (A) $[\text{CuL}_1]\cdot 2\text{H}_2\text{O}$ (1), (B) $[\text{MnL}_1]\cdot 4\text{H}_2\text{O}$ (2), (C) $[\text{NiL}_1]\cdot 3\text{H}_2\text{O}$ (3), (D) $[\text{ZnL}_1]\cdot 5\text{H}_2\text{O}$ (4), (E) $[\text{CuL}_2]\cdot 4\text{H}_2\text{O}$ (5), (F) $[\text{MnL}_2]\cdot 3\text{H}_2\text{O}$ (6), (G) $[\text{NiL}_2]\cdot 4\text{H}_2\text{O}$ (7), (H) $[\text{ZnL}_2]\cdot 4\text{H}_2\text{O}$ (8), (I) $[\text{CuL}_3]\cdot 3\text{H}_2\text{O}$ (9), (J) $[\text{MnL}_3]\cdot 4\text{H}_2\text{O}$ (10), (K) $[\text{NiL}_3]\cdot 2\text{H}_2\text{O}$ (11), and (L) $[\text{ZnL}_3]\cdot 3\text{H}_2\text{O}$ (12).

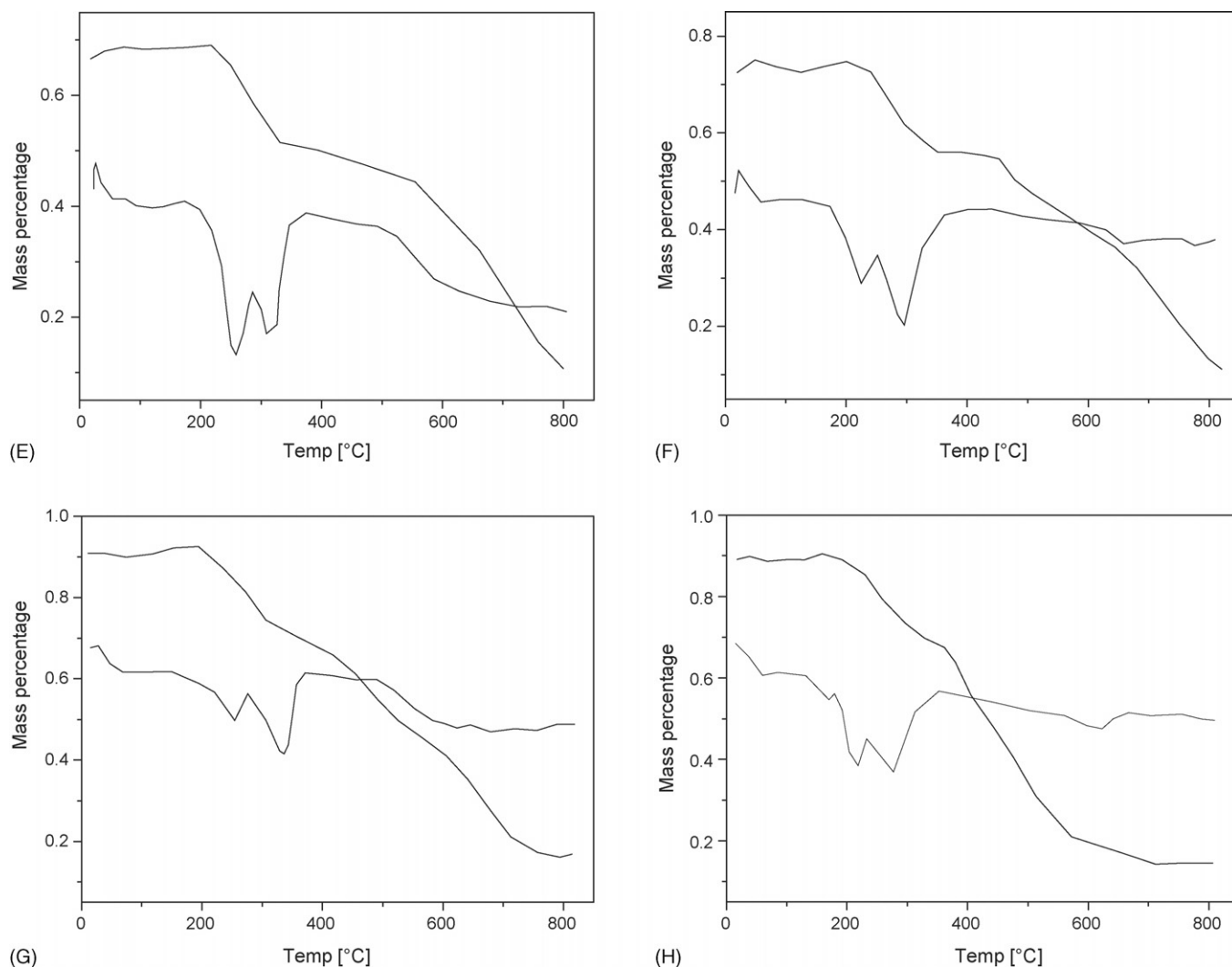


Fig. 12. (Continued)

3.6. X-ray powder diffraction

X-ray powder diffraction patterns in the $5^\circ < 2\theta < 90^\circ$ of the compounds were carried in order to obtain an idea about the lattice dynamics of the compound. By comparison of the obtained X-ray powder diffraction patterns shown in Fig. 10, the X-ray powder diffraction pattern throws light only on the fact that each solid represents a definite compound of a definite structure which is not contaminated with starting materials. This identification of the complexes was done by the known method [29]. Such facts suggest that the prepared compounds are amorphous.

3.7. Scanning electron microscopy

Purity and morphology of the complexes obtained were studied by SEM. The obtained SEM micrographs, shown in Fig. 11, allow to verify that the copper, manganese, nickel, and zinc(II) complexes are the ones with the well-formed amorphous shape. Such facts are in agreement with the obtained X-ray results.

Single crystals of the complexes could not be isolated from any solutions; thus, no definitive structure can be described. However, the spectroscopic data and elemental analysis of CHN enable us to predict possible structures (1–10).

3.8. Thermal studies

The thermal degradation of all the metal complexes (1–12) was studied using thermogravimetric techniques and a temperature range of 25–800 °C (Fig. 12). The thermal stability data are listed in Table 4. The data from the thermogravimetric analysis clearly indicated that the decomposition of the complexes proceeds in two or three steps. Water molecules were lost in between 50 and 300 °C and metal oxides were formed above 600 °C for Cu(II), Mn(II), Ni(II), and Zn(II) complexes. For these complexes, the removal of water can proceed in two steps. All complexes lost hydration water between 50 and 300 °C, and then the coordinated water molecule was lost above ≥ 300 °C. The decomposition was complete at ≥ 600 °C for all complexes. The degradation pathway for all complexes may be represented

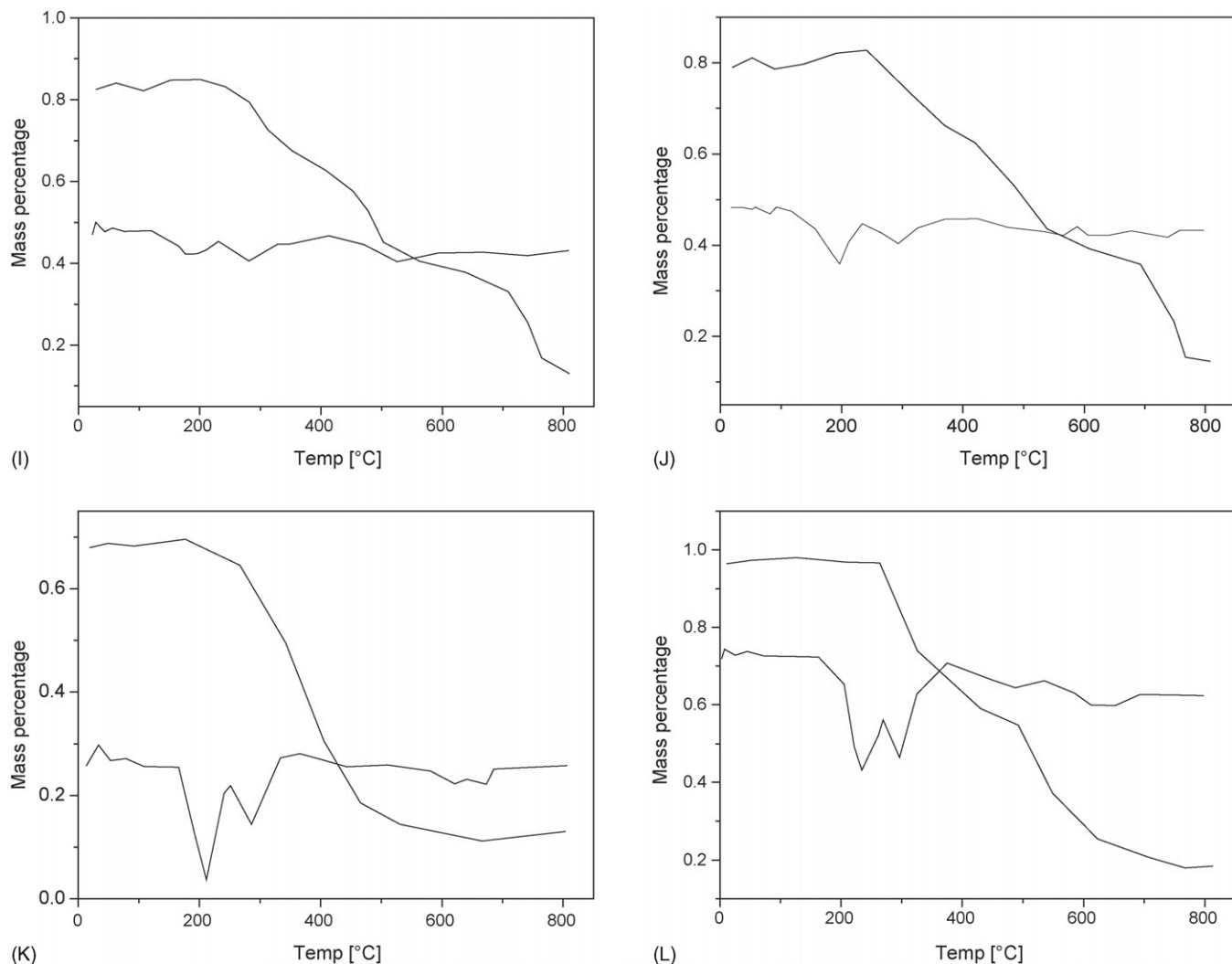
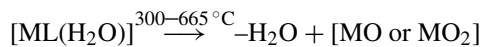
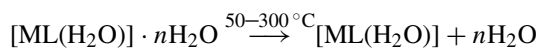


Fig. 12. (Continued).

as follows:



where MO = CuO, NiO, ZnO; MO₂ = MnO₂.

References

- [1] X. Tai, X. Yin, Q. Chen, M. Tan, *Molecules* 8 (2003) 439.
- [2] M. Sonmez, A. Levent, M. Sekerci, *Russ. J. Coord. Chem.* 30 (9) (2004) 655.
- [3] M. Tuncel, S. Serin, *Synth. React. Inorg. Met. Org. Nano Met. Chem.* 35 (2005) 203.
- [4] A.A. Khandar, K. Nejati, Z. Rezvani, *Molecules* 10 (2005) 302.
- [5] A.D. Garnovskii, I.S. Vasilchenko, *Russ. Chem. Rev.* 71 (2002) 943.
- [6] A.D. Garnovskii, A.L. Nivorozhkin, V.I. Minkin, *Coord. Chem. Rev.* 126 (1993) 1.
- [7] F.D. Karia, P.H. Parsania, *Asian J. Chem. Soc.* 11 (3) (1999) 991.
- [8] P.G. More, R.B. Bhalvankar, S.C. Pattar, *J. Indian Chem. Soc.* 78 (9) (2001) 474.
- [9] A.H. El-masry, H.H. Fahmy, S.H.A. Abdelwahed, *Molecules* 5 (2000) 1429.
- [10] M.A. Baseer, V.D. Jadhav, R.M. Phule, Y.V. Archana, Y.B. Vibhute, *Orient. J. Chem.* 16 (3) (2000) 533.
- [11] S.N. Pandeya, D. Sriram, G. Nath, E. De Clercq, *IL Farmaco* 54 (1999) 624.
- [12] W.M. Singh, B.C. Dash, *Pesticides* 22 (11) (1988) 33.
- [13] E.M. Hodnett, W.J. Dunn, *J. Med. Chem.* 13 (1970) 768.
- [14] S.B. Desai, P.B. Desai, K.R. Desai, *Heterocycl. Commun.* 7 (1) (2001) 83.
- [15] P. Pathak, V.S. Jolly, K.P. Sharma, *Orient. J. Chem.* 16 (1) (2000) 161.
- [16] S. Samadhiya, A. Halve, *Orient. J. Chem.* 17 (1) (2001) 119.
- [17] F. Aydogan, N. Ocal, Z. Turgut, C. Yolacan, *Bull. Korean Chem. Soc.* 22 (2001) 476.
- [18] A.E. Taggi, A.M. Hafez, H. Wack, B. Young, D. Ferraris, T. Lectka, *J. Am. Chem. Soc.* 124 (2002) 6626.
- [19] K. Hansongnern, S. Tempiam, J.C. Liou, F.L. Laio, T.H. Lu, *Anal. Sci.* 19 (2003) x13.
- [20] P.L. Coort, M. Johansson, *Electroanalysis* 12 (2000) 565.
- [21] D. Choi, S.K. Lee, T.D. Chung, H. Kim, *Electroanalysis* 12 (2000) 477.
- [22] P. Alka, P. Vinod, V.S. Jolly, *Orient. J. Chem.* 10 (1) (1994) 73.
- [23] A. Halve, A. Goyal, *Orient. J. Chem.* 12 (1) (2001) 87.
- [24] A.A. Khandar, Z. Rezvani, *Polyhedron* 18 (1999) 129.

- [25] R.J. Fessenden, J.S. Fessenden, *Inorganic Chemistry*, vol. 13, fourth ed., Cole Publishing Company, California, 1990, pp. 587–648.
- [26] M. Mikuraya, T. Sasaki, A. Anjiki, S. Ikemoe, T. Tokh, *Bull. Chem. Soc. Jpn.* 65 (1992) 334.
- [27] G.G. Mohamed, *Spectrochim. Acta Part A* 57 (2001) 411.
- [28] H. Koksal, M. Tumer, S. Seria, *Synth. React. Inorg. Met. Org. Chem.* 26 (1996) 1577.
- [29] B.D. Cullity, *Elements of X-ray Diffraction*, second ed., Addison-Wesley Inc., 1993.